Letter

Emergence of partially disordered antiferromagnetism and isothermal magnetization plateau due to geometrical frustration in a metallic compound, Er_2RhSi_3

Kartik K. Iyer,[1,2,*] Kalobaran Maiti,[1] Sudhindra Rayaprol,[3] Ram Kumar,[4] S. Mattepanavar,[5] S. Dodamani,[2] and E. V. Sampathkumaran[6,†]

[1]*Tata Institute of Fundamental Research, Homi Bhabha Road, Colaba, Mumbai 400005, India*
[2]*KLE Society's Dr. Prabhakar Kore Basic Science Research Centre, KLE Academy of Higher Education and Research, Belagavi 590010, India*
[3]*UGC-DAE Consortium for Scientific Research, Mumbai Centre, BARC Campus, Trombay, Mumbai 400085, India*
[4]*Maryland Quantum Materials Center, University of Maryland, College Park, Maryland 20742, USA*
[5]*KLE Society's Basavaprabhu Kore Arts, Science and Commerce College, Chikodi 591201, India*
[6]*Homi Bhabha Centre for Science Education, TIFR, V. N. Purav Marg, Mankhurd, Mumbai 400088, India*

(Received 16 June 2023; accepted 14 September 2023; published 10 October 2023)

Partially disordered antiferromagnetism (PDA) (in which one of the three magnetic ions in a triangular network remains magnetically disordered) has been known commonly among geometrically frustrated insulating materials. The 1/3 plateau in isothermal magnetization M of such materials has been of great theoretical interest. Here we report these properties in an AlB_2-structure-derived metallic material, Er_2RhSi_3, in which the Er sublattice has triangular networks. The presence of a well-defined λ anomaly in the temperature T dependence of heat capacity and its magnetic-field H dependence and the loss of spin-disorder contribution to electrical resistivity ρ confirm antiferromagnetic order below $T_N = 5$ K. On the other hand, the separation of zero-field-cooled and field-cooled dc magnetic susceptibility χ curves, the decay of isothermal remnant magnetization, and the frequency dependence of real and imaginary components of ac χ suggest the onset of spin-glass freezing concomitant with the antiferromagnetic order. In addition, interestingly, we observe the 1/3 plateau in $M(H)$ below 20 kOe for $T < T_N$. The change in ρ as a function of H at a given temperature well below T_N is also revealing, with this compound exhibiting a plateau below 20 kOe, with complexities at higher fields. Therefore, this compound serves as a prototype for theoretical understanding of transport behavior across the 1/3 plateau due to PDA magnetism in a metal without any interference from the $4f$ delocalization phenomenon.

DOI: 10.1103/PhysRevMaterials.7.L101401

The phenomenon of highly frustrated magnetism due to the geometrical arrangement of the magnetic ions, referred to as geometrically frustrated (GF) magnetism, is one of the modern topics of research in condensed matter physics, as such a frustration has been known to lead to a variety of interesting magnetic states [1–9]. This article essentially focuses on two of these aspects, viz., partially disordered antiferromagnetism (PDA) and magnetization plateaus. The concept of PDA magnetism was originally invoked to describe a situation for materials containing a triangular magnetic framework, in which the magnetic ions at two vertices are antiferromagnetically coupled, while the third one is left random due to geometrical frustration [1,2]. This kind of magnetism has been of interest due to the fact that all the magnetic ions are crystallographically equivalent yet exhibiting different magnetic behavior. Very early examples for PDA magnetism are $CsCoCl_3$ and $CsCoBr_3$ [1,2], and during the past two decades Ca_3CoRhO_6 [3–5] and $Ca_3Co_2O_6$ [6–8] have been attracting attention. With respect to the magnetization plateaus, this is in general a subject of considerable theoretical and experimental investigation in terms of Shastry-Sutherand, square, kagome, and triangular insulating systems, as multiple plateaus can arise not only due to GF magnetism, but also due to various other magnetic interaction frustrations (see, for instance, Refs. [9–12]). Quantum effects have been shown to play a major role. The PDA magnetism arising from GF magnetism in triangular magnetic lattices is often characterized, in particular, by a plateau at 1/3 of the saturation magnetization M. There has been a flurry of activity in recent years studying this 1/3 plateau in, e.g., $Ba_3NiSb_2O_9$, $Ba_3NiNb_2O_9$ [13,14], volborthite [15], Cs_2CoBr_4 [16], $CoGeO_3$ [17], and $Cu_3Bi(TeO_3)_2O_2Cl$ [18]. Readers may also refer to the seminal theoretical work by Chubukov and Golosov [19]. Such plateaus occur irrespective of the spin value of the magnetic ion (see, for instance, [11,12,17–33] and references therein). Besides many such insulators, a semiconducting triangular system Eu_3InAs_3 has been reported very recently [34].

Clearly, the identification of materials exhibiting such quantized steps, in particular the 1/3 plateau, is an important direction of research in the field of GF magnetism. Obviously, any kind of PDA magnetic structure, even in other GF families, is of great interest in condensed matter physics, e.g., $Gd_2Ti_2O_7$ [35]. However, such reports in a metallic environment are scarce and sporadic, e.g., UNi_4B [36], CePdAl [37], $Tb_3Ru_4Al_{12}$ [38], and very recently $EuRh_2Al_8$ [39]. The compound $TbRh_6Ge_6$ [40] has been recently

*Iyerkk@gmail.com
†sampathev@gmail.com

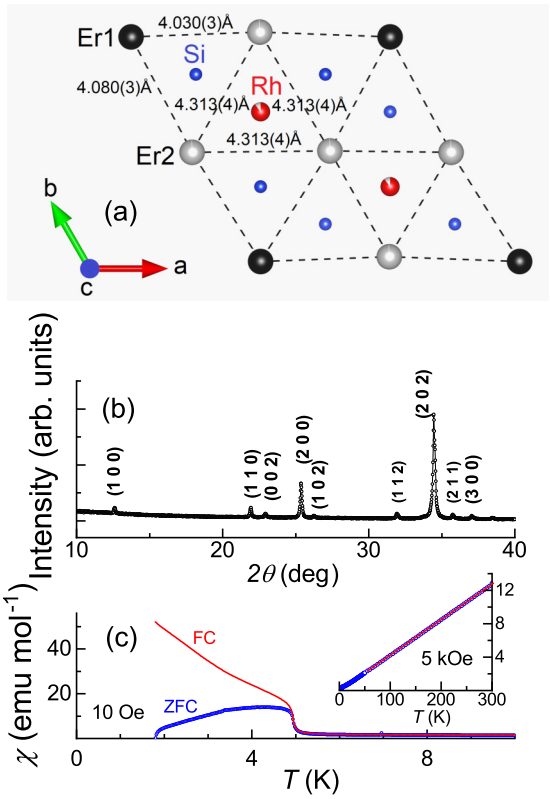

FIG. 1. (a) Unit cell of Er_2RhSi_3 viewed along the c axis, showing triangular arrangement of Er ions in the Er layer; intralayer distances between Er atoms are given. An adjacent Rh-Si layer is also shown. (b) X-ray-diffraction pattern (Cu K_α) below $2\theta = 40^\circ$ to show weak superstructure lines (100) and (110). (c) Magnetic susceptibility as a function of temperature below 10 K for the zero-field-cooled and field-cooled conditions of the specimens, measured with 10 Oe. The inset shows the inverse χ in a field of 5 kOe, with a straight line through the Curie-Weiss regime.

reported to show a 1/9 plateau, in addition to a 1/3 plateau. The question therefore arises whether the Rudermann-Kittel-Kasuya-Yosida (RKKY) indirect exchange interaction usually mediating magnetic ordering in metals, in particular among rare-earth metals R, is not generally favorable to cause these features of geometric frustration. It is therefore of great interest to search for materials, without interference from other exotic phenomena due to f-electron delocalization (as in CePdAl [37]), exhibiting features characteristic of PDA magnetism and the 1/3 plateau to provide relatively simple examples to enable the theorists to work further in this direction. In this article we present evidence of such magnetic characteristics in Er_2RhSi_3, derived from an AlB_2-derived hexagonal structure [41].

A good number of ternary rare-earth compounds of the type $R_2(T)X_3$ (where T is a transition metal ion in this paragraph and $X = Si$ or Ge) have been derived from an AlB_2 hexagonal crystal structure. The sites for T and X are $4f$ and $12i$, respectively forming T-X layers. The layers of T-X form a honeycomb network and the layers of the triangular network of R ions [Fig. 1(a)] alternate with T-X in the c direction. In the event of the ordered replacement of the boron site by T and X, two types of rare-earth compounds, viz., $2b$ and $6h$, can be visualized depending on whether the nearest hexagons in the adjacent layers contain ordered T-X or X atoms. As a result of this difference in the chemical surrounding, the interatomic distances undergo subtle differences, as discussed in Ref. [42] for Er_2RhSi_3 [and shown in Fig. 1(a) for Er-Er distances]. This is presumably responsible for doubling of the unit-cell parameters with respect to those expected for the disordered distribution of T and X [in which case the chemical formula can be written as $R(T)_{0.5}X_{1.5}$]. For crystallographic details, the readers are referred to Ref. [41] and the Supplemental Material [42]. Among these, many novel magnetic and transport anomalies have been reported (see references in [43–56]) for the past three decades for several members of the R_2PdSi_3 family. The most notable one is Gd_2PdSi_3, the transport anomalies of which include Kondo-like electrical resistivity ρ [46]; it is intriguing that Hall anomaly typical of the topological Hall effect was reported two decades ago, long before this concept was recognized in metals, as noted in Ref. [49]. Gd_2PdSi_3 is the first centrosymmetric case to exhibit magnetic skyrmion behavior [48,50–52], strongly modulated by the Pd/Si superlattice [51]. Therefore, it is important to investigate Rh analogs. Other than some initial studies long ago [41,57,58], in particular on the Ce case in depth [59–67], Gd, Tb, and Dy members [68] are special as these exhibit magnetic and transport properties comparable to those of Gd_2PdSi_3. The properties of the isomorphic Er compound [69] presented in this paper reveal uniqueness in the context of PDA magnetism and one-third magnetization plateau.

A polycrystalline sample was prepared by melting together stoichiometric amounts of constituent elements in an arc furnace in an atmosphere of argon under partial pressure, followed by annealing at 1073 K for about a week in an evacuated sealed quartz tube. The x-ray-diffraction pattern (recorded with Cu K_α radiation) was analyzed by the Rietveld refinement method, which confirmed the single-phase nature of molten ingot (see the Supplemental Material [42]). The pattern was found to be in excellent agreement with that of Ref. [41], including the appearance of superstructure lines [Fig. 1(b)] establishing doubling of the unit-cell parameters ($a = \sim 8.1043$ and $c = \sim 7.7518$ Å). Details of the temperature T and magnetic-field H dependences of ac and dc M, heat-capacity C, and electrical resistivity ρ measurements can be found in Ref. [42].

In the inset of Fig. 1(c) we show the T dependence of the inverse susceptibility χ obtained in a field of 5 kOe. The plot is found to be linear over a wide T range well above 10 K. The effective moment $\mu_{\rm eff}$ obtained from the slope of the plot (approximately $9.7\mu_B$) is the same as the theoretical value of $9.7\mu_B$ for trivalent Er ions. The paramagnetic Curie temperature is found to be approximately 1.4 K; the positive sign is indicative of ferromagnetic correlations between Er ions, which is different from other rare-earth cases in the same family [68]. We note that, as the temperature is lowered, there is an upturn of χ around 5 K beyond the value expected from the high-temperature Curie-Weiss behavior followed by a peak, as though antiferromagnetic ordering sets in, as shown in Fig. 1(c) for the 10 Oe measuring field. The zero-field-cooled (ZFC) and field-cooled (FC) curves for this low field tend to deviate from each other at the onset of magnetic

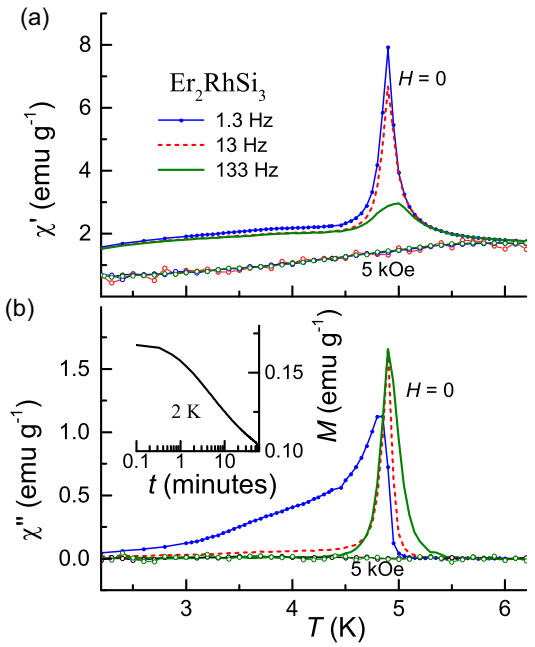

FIG. 2. (a) Real and (b) imaginary parts of ac susceptibility of Er_2RhSi_3 below 6 K, obtained with different frequencies in zero field as well as in 5 kOe. The curves for 5 kOe for all frequencies overlap and are featureless. The inset shows isothermal remnant magnetization at 2 K.

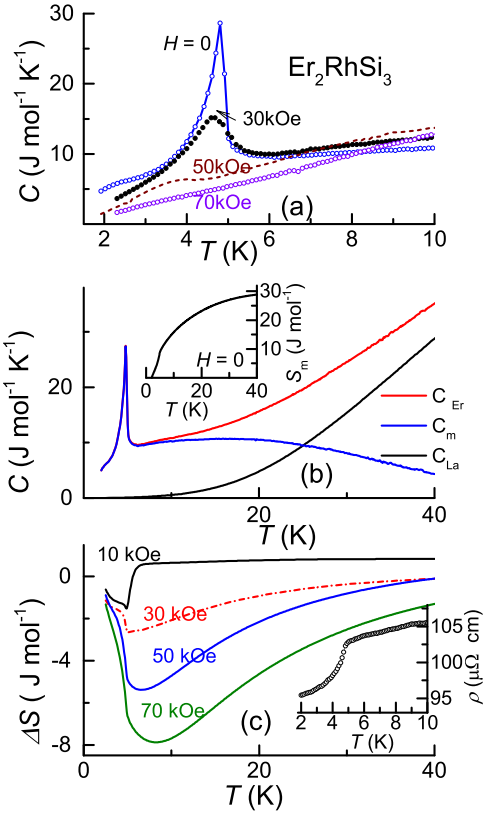

FIG. 3. (a) Zero-field and in-field heat capacity below 10 K and (b) zero-field heat capacity in a wider temperature range of 2–40 K for Er_2RhSi_3. (b) Magnetic contribution to heat capacity C_m for Er_2RhSi_3, employing the heat capacity of La_2RhSi_3 (also shown) for the nonmagnetic part, along with the magnetic entropy S_m curve, derived from C_m versus T for the Er sample in the inset. (c) Isothermal entropy change curves as a function of temperature (see the text for details) for different final fields starting from zero field; the inset shows the electrical resistivity data at low temperatures.

order itself, with the FC curve continuing to rise down to 2 K, typical of spin glasses in many concentrated magnetic materials [38,70,71]. For another interesting χ behavior in the vicinity of the T region of 2–20 K at low fields (20, 50, and 100 Oe), readers are referred to the Supplemental Material [42].

In order to explore further the origin of the above features, we have measured ac χ in the low-temperature region with frequencies 1.3, 13, 133, and 1333 Hz; the results obtained as a function of T in the vicinity of the magnetic transition are shown in Fig. 2. The curves are featureless at higher temperatures. It is apparent from this figure that not only the real part χ' but also the imaginary part χ'' exhibits prominent peaks in magnitude, with the sharp upturn occurring at 5 K, as expected for spin glasses [72]. There is a weak frequency υ dependence of the peak temperature, say, in χ', that is, 0.2 K for a variation of υ from 1.3 to 133 Hz. (The peak values also undergo a decrease with increasing υ, with significant suppression for 1333 Hz, which is curious). The peaks vanish for a small application of a dc magnetic field (say, 5 kOe), as revealed by the flatness of the plot in the figure. The results establish that this compound undergoes spin-glass freezing. The most notable observation, as inferred from the peak temperature in χ', is that the spin freezing occurs exactly at the onset of magnetic ordering. In order to render further support to the existence spin-glass freezing, we have measured isothermal remnant magnetization $M_{\rm IRM}$ as a function of time t at 2 K. This curve, shown in the inset of Fig. 2, was obtained as follows: After zero-field cooling of the specimen at 2 K, the specimen was left in a magnetic field of 5 kOe for 5 min; immediately after switching off the field, $M_{\rm IRM}$ was measured as a function of t for about an hour. From the inset of Fig. 2 it is clear that there is a slow decay of $M_{\rm IRM}$, varying essentially logarithmically with t (barring slower decay for a few initial seconds), consistent with what is expected for spin glasses.

Having established the onset of spin-glass freezing at 5 K, support for long-range magnetic order pointing to a well-defined magnetic structure comes from the $C(T)$ data, apart from the appearance of magnetic Bragg peaks in the neutron diffraction data [57]. We show the $C(T)$ data in the T region of interest only (much less than 10 K) in Fig. 3(a), as there is no worthwhile feature measured up to 150 K. It is evident from Fig. 3(a) that the zero-field data exhibit a strong λ anomaly with a sharp upturn at 5 K. This is a characteristic feature of long-range magnetic ordering arising from a well-defined magnetic structure. Spin-glass freezing alone would have resulted in smearing of the feature at the onset of freezing. Therefore, viewed together with the features in the ac and dc magnetization presented above, this establishes that spin-glass freezing and a well-defined magnetic structure set in essentially at the same temperature, namely, at 5 K. With respect to the behavior in the presence of external fields, there is a gradual smearing and broadening of the peak and the

peak moves towards a lower temperature, for example, for 30 and 50 kOe to 4.5 and 3.8 K, respectively. This establishes that the strong λ anomaly arises from antiferromagnetism. In short, these results establish that PDA magnetism occurs at the magnetic ordering temperature of $T_N = 5$ K. Finally, we have also derived the magnetic contribution C_m to $C(T)$ by measuring $C(T)$ of the La analog as in Ref. [68], which is shown in Fig. 3(b). The magnetic entropy S_m [Fig. 3(b), inset] obtained by integrating C_m/T versus T is approximately 8 J/mol K at T_N. If one assumes that the magnetic ordering arises from the crystal-field-split doublet ground state (as Er^{3+} is a Kramers ion), the minimum expected value for the magnetic entropy at T_N should be $2R\ln 2 = 11.52$ J/mol K. Therefore, the observed lower value supports that a significant fraction of Er ions are magnetically disordered. It may be remarked that the theoretical value of magnetic entropy for full degeneracy of the $4f$ orbital of Er^{3+} (for which the total orbital angular momentum is $J = 15/2$) is equal to $(2R\ln 16 =)46.1$ J/mol K, which is far above the observed value at T_N. Clearly, crystal-field splitting of the $4f$ orbital is present, which is also supported by a similar lower value of magnetic moment determined by neutron diffraction [57].

We have derived the isothermal entropy change, defined as $\Delta S = S(H)$–$S(0)$, from the area under the curves of C/T versus T, measured at different fields, and the results obtained are shown in Fig. 3(c). The curves fall in the negative quadrant with a negative peak, typical of a dominant ferromagnetic component in such fields [73]. This demonstrates field-induced changes in the magnetic structure in the magnetically ordered state. The peak values are reasonably large, say, for 0–50 kOe field variation, with the curve spreading over a wide T range above T_N. Surprisingly, ΔS changes sign sharply at the loss of magnetic order above 5 K for 10 kOe, and the positive sign above T_N implies possible field-induced magnetic fluctuations in such low fields. The sign becomes negative in the paramagnetic state for $H > 10$ kOe as expected, but the large magnitude over a wide T range may be due to the antiferromagnetic clusters giving rise to an effective ferromagnetic alignment. The results overall imply that this compound may be an example of interesting magnetic precursor effects [46,47,73–75] in the paramagnetic state, which has also been addressed theoretically in recent times [47,76,77].

We present isothermal magnetization behavior for 1.8, 4, and 6 K in Figs. 4(a)–4(c) to reveal the 1/3 plateau. There is a sharp rise at 1.8 K for the application of an initial small H and there is a plateau immediately thereafter until 20 kOe. The sharpness of these features is a bit smeared in the 4 K plot. There is an upturn near about 20 kOe after the plateau and the variation is weak beyond about 30 kOe. The plot of $M(H)$ tends to flatten, varying weakly beyond 60 kOe until the measured field of 120 kOe [Fig. 4(a), inset], as though there is a tendency to saturate. All these $M(H)$ curves are found to be nonhysteretic. A linear extrapolation of the high-field curve to zero field yields a value of about $6.5\mu_B$ per Er ion. This value is far below the saturation value expected for fully degenerate trivalent Er ions ($9\mu_B$ per Er ion) and so the reduced value can be attributed to a decrease in the magnetic moment and possible strong anisotropy resulting from crystal-field effects. The most intriguing observation relevant to the aim of this article is that the value of the similarly extrapolated magnetic

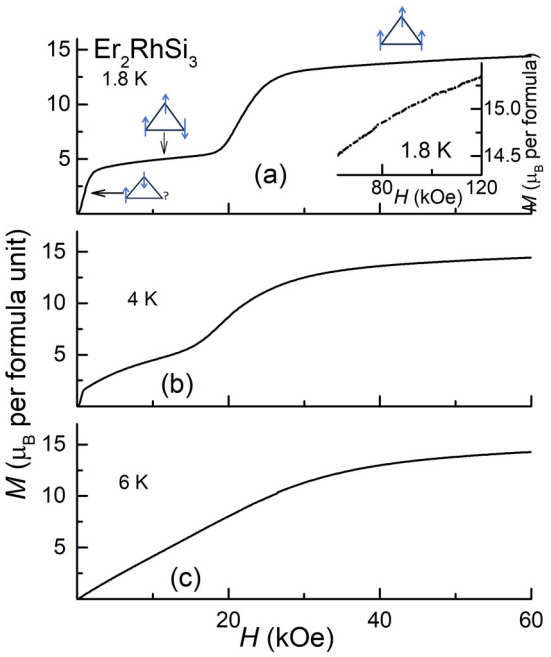

FIG. 4. Isothermal magnetization of Er_2RhSi_3 below 60 kOe at (a) 1.8, (b) 4, and (c) 6 K for the forward variation of the magnetic field. The inset shows the behavior in the range 60–120 kOe at 1.8 K. Also shown in (a) is a schematic representation of a scenario [5] for the orientation of magnetic moments in a triangular network; the question mark represents magnetically disordered ions.

moment in the plateau region is approximately $2.15\mu_B$ per Er ion, which is essentially one-third of the extrapolated value from the high-field data (obtained above). A simple picture for the origin of 1/3 magnetization plateau, advanced for a triangular lattice $Ca_3Co_2O_6$ [5] is as follows: The magnetic ion at one of the three vortices of the triangle is magnetically disordered as evidenced by spin-glass features discussed above, while the other two are coupled antiparallel in zero field in the virgin state; in the plateau region, the magnetic moment of the disordered magnetic ion gets oriented along the field, leaving the other two aligned antiparallel to each other, leading to a ferrimagnetic state. It is not straightforward to understand why such an intermediate state is stable against perturbation by a magnetic field, in our case, up to 20 kOe; presumably, the antiparallel interaction is too strong to flip the moments of Er with this external field. Beyond 30 kOe, all three sites tend to align ferromagnetically, resulting in three times the magnetic moment of the plateau region. For the sake of the reader, a schematic representation of this scenario is shown for a triangle in Fig. 4. Thus, the 1/3 isothermal magnetization plateau could be consistently interpreted with the idea of partially disordered antiferromagnetism. Note that the plateau vanishes as soon as the long-range magnetic order regime is crossed, as seen for the $M(H)$ curve for 6 K.

Previous neutron diffraction studies [57] suggest that there is no crystal structure change in the magnetically ordered state. In that work, both Er ions are assumed to carry an equal magnetic moment of $5.9\mu_B$ per Er ion, which is below the value of $9\mu_B$ for the fully $4f$-degenerate trivalent Er ion, suggesting the presence of crystal-field splitting. We would

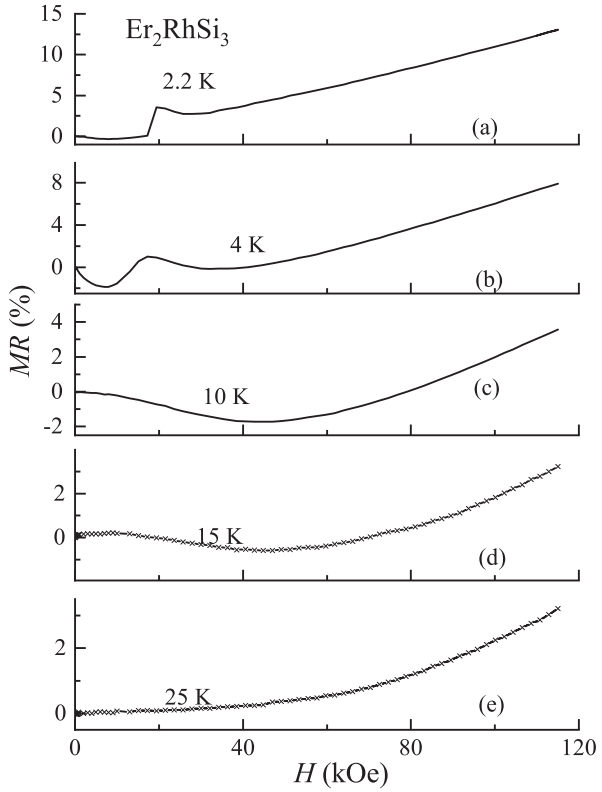

FIG. 5. Isothermal magnetoresistance, defined as $[\rho(H) - \rho(0)]/\rho(0)$, for Er_2RhSi_3, at (a) 2.2, (b) 4, (c) 10, (d) 15, and (e) 25 K.

like to state that it is difficult to reconcile the PDA magnetic structure proposed here with the conclusions obtained from these neutron diffraction studies. It is not uncommon, particularly within this ternary family, that reinvestigations by modern facilities and/or better quality samples have yielded results contradicting previous magnetic structure proposals, for example, for Tb_2PdSi_3 [78,79] and for Nd_2PdSi_3 [44,78]. Besides, a PDA system would be characterized by a broad background below the sharp magnetic peaks, suggestive of quasielastic peaks arising from spin-glass component, as in Ca_3CoRhO_6 [80,81]. A careful look at the background below the intense peaks in the reported neutron diffraction pattern [57] indeed provides an indication of the same. In view of these findings, we call for detailed neutron diffraction studies to search for some kind of PDA magnetic structure, before attaching any significance to the apparent discrepancy with the present conclusion.

We now demonstrate the behavior of magnetoresistance (in the transverse geometry) across the $1/3$ plateau regime in this metallic system, serving as a subject warranting further theoretical work to understand transport anomalies in the $1/3$ plateau regime, as such an opportunity is not provided by insulating PDA systems. The $\rho(T)$ plot [see Fig. 3(c), inset] shows distinct evidence for the loss of the spin-disorder contribution to ρ at T_N. Figures 5(a)–5(e) show the behavior of isothermal magnetoresistance (MR) at various temperatures across T_N. Here MR is defined as $[\rho(H) - \rho(0)]/\rho(0)$. The curves are essentially nonhysteretic. Looking at the MR curve at 2.2 K [see Fig. 5(a)], the magnitude is negligibly small below 20 kOe, but a negative sign emerges after a small change in applied H (possibly due to grain boundaries or spin-glass component); it is notable that MR otherwise is almost flat in the $1/3$ magnetization plateau region, as though magnetism is topologically protected, apparently avoiding even conventional magnetic and nonmagnetic contributions for the scattering process. After this plateau region is crossed, there is a distinct upturn to the positive quadrant, followed by a weak drop around 30 kOe, possibly due to the ferromagnetic alignment contribution. With a further increase of H, that is, in the region where there is a tendency for magnetization to saturate, MR surprisingly keeps increasing, remaining in the positive quadrant. Such a linear MR variation in the essentially ferromagnetically aligned state is puzzling (as ferromagnets are usually characterized by negative MR with a nonlinear dependence on H). It is not clear whether the classical contribution due to conduction electrons dominates the ferromagnetic contribution at higher fields, leading to positive MR. At 4 K, the features are similar, except that the initial drop is more prominent. Just above T_N, say, at 10 K, there is a competition between the well-known paramagnetic contribution (negative sign with an H^2 dependence) and the positive classical contribution, leading to a minimum at the intermediate-field range. With increasing T, since the paramagnetic contribution should gradually weaken, the minimum gradually vanishes, as shown for 10, 15, and 25 K [Figs. 5(c)–5(e)].

In conclusion, we have reported the results of our bulk measurements on Er_2RhSi_3 containing essentially localized $4f$ electrons in a triangular network, hitherto not paid much attention in the literature. A fascinating finding is that this compound exhibits characteristic features of PDA magnetism, also characterized by the $1/3$ magnetization plateau in this case, in a material with RKKY interaction, that too without any interference from other $4f$-related phenomena (like the Kondo effect typical of Ce or U systems). It may be remarked that none of the isostructural ternary rare-earth compounds has been known to show such PDA characteristics in the past, in particular, other rare-earth compounds of this Rh family (R = Gd, Tb, Dy, and Ho) [68,69] as well as the Er counterpart in the Pd-based family, Er_2PdSi_3 [56]. This is puzzling and renders support to the conclusion that this compound is a unique magnetic material, possibly suggesting an interesting magnetic interaction between the orientated crystal-field-split ground state of the $4f$ orbital of Er with the Rh $4d$ orbital and therefore it is worth probing this aspect further. Finally, this compound may also serve as a prototype for transport behavior across the $1/3$ magnetization plateau.

The authors acknowledge financial support from the Department of Atomic Energy (DAE), Government of India (Project No. RTI4003, DAE OM No. 1303/2/2019/R&D-II/DAE/2079). E.V.S. is grateful to the Department of Atomic Energy, Government of India, for financial support through a Raja Ramanna Fellowship. K.M. is grateful for financial support from BRNS, DAE under the DAE-SRC-OI program. S.M. is grateful for support from Vision Group on Science and Technology–GRD through Grant No. 852.

[1] M. Mekata, J. Phys. Soc. Jpn. **42**, 76 (1977).

[2] W. B. Yelon, D. E. Cox, and M. Eibschutz, Phys. Rev. B **12**, 5007 (1975).

[3] S. Niitaka, H. Kageyama, M. Kato, K. Yoshimura, and K. Kosuge, J. Solid State Chem. **146**, 137 (1999); S. Niitaka, H. Kageyama, K. Yoshimura, K. Kosuge, S. Kawano, N. Aso, A. Mitsuda, H. Mitamura, and T. Goto, J. Phys. Soc. Jpn. **70**, 1222 (2001).

[4] E. V. Sampathkumaran and A. Niazi, Phys. Rev. B **65**, 180401(R) (2002).

[5] H. Kageyama, K. Yoshimura, K. Kosuge, H. Mitamura, and T. Goto, J. Phys. Soc. Jpn. **66**, 1607 (1997).

[6] A. Maignon, C. Michel, A. C. Masset, C. Martin, and B. Raveau, Eur. Phys. J. B **15**, 657 (2000).

[7] S. Rayaprol, K. Sengupta, and E. V. Sampathkumaran, Solid State Commun. **128**, 79 (2003).

[8] F. Levy, I. Sheikin, C. Berthier, M. Horvatic, M. Takigawa, H. Kageyama, T. Waki, and Y. Ueda, Europhys. Lett. **81**, 67004 (2008).

[9] For a recent review on quantum spin liquids see V. R. Shaginyan, V. A. Stephanovich, A. Z. Msezane, G. S. Japaridze, J. W. Clark, M. Y. Amusia, and E. V. Kirichenko, J. Mater. Sci. **55**, 2257 (2020).

[10] H. O. Jeschke, H. Nakano, and T. Sakai, Phys. Rev. B **99**, 140410(R) (2019).

[11] D. Flavián, J. Nagl, S. Hayashida, M. Yan, O. Zaharko, T. Fennell, D. Khalyavin, Z. Yan, S. Gvasaliya, and A. Zheludev, Phys. Rev. B **107**, 174406 (2023).

[12] Z. W. Ouyang, Y. C. Sun, J. F. Wang, X. Y. Yue, R. Chen, Z. X. Wang, Z. Z. He, Z. C. Xia, Y. Liu, and G. H. Rao, Phys. Rev. B **97**, 144406 (2018).

[13] Y. Shirata, H. Tanaka, T. O. A. Matsuo, K. Kindo, and H. Nakano, J. Phys. Soc. Jpn. **80**, 093702 (2011).

[14] J. Hwang, E. S. Choi, F. Ye, C. R. Dela Cruz, Y. Xin, H. D. Zhou, and P. Schlottmann, Phys. Rev. Lett. **109**, 257205 (2012).

[15] H. Ishikawa, M. Yoshida, K. Nawa, M. Jeong, S. Krämer, M. Horvatić, C. Berthier, M. Takigawa, M. Akaki, A. Miyake *et al.*, Phys. Rev. Lett. **114**, 227202 (2015).

[16] L. Facheris, K. Y. Povarov, S. D. Nabi, D. G. Mazzone, J. Lass, B. Roessli, E. Ressouche, Z. Yan, S. Gvasaliya, and A. Zheludev, Phys. Rev. Lett. **129**, 087201 (2022).

[17] H. Guo, L. Zhao, M. Baenitz, X. Fabrèges, A. Gukasov, A. Melendez Sans, D. I. Khomskii, L. H. Tjeng, and A. C. Komarek, Phys. Rev. Res. **3**, L032037 (2021).

[18] X. Liu, Z. Ouyang, D. Jiang, J. Cao, T. Xiao, Z. Wang, Z. Xiao, and W. Tong, J. Magn. Magn. Mater. **565**, 170228 (2023).

[19] A. V. Chubukov and D. I. Golosov, J. Phys.: Condens. Matter **3**, 69 (1991).

[20] A. Farchakh, A. Boubekri, and M. El Hafidi, J. Low Temp. Phys. **206**, 131 (2022).

[21] T. Sakai, K. Okamoto, and T. Tonegawa, Phys. Rev. B **100**, 054407 (2019).

[22] Y. Kamiya, L. Ge, Tao Hong, Y. Qiu, D. L. Quintero-Castro, Z. Lu, H. B. Cao, M. Matsuda, E. S. Choi, C. D. Batista, M. Mourigal, H. D. Zhou, and J. Ma, Nat. Commun. **9**, 2666 (2018).

[23] M. E. Zhitomirsky, A. Honecker, and O. A. Petrenko, Phys. Rev. Lett. **85**, 3269 (2000).

[24] K. Hida and I. Affleck, J. Phys. Soc. Jpn. **74**, 1849 (2005).

[25] *Magnetization Plateaus*, edited by C. Lacroix, P. Mendels, and F. Mila (Springer, Heidelberg, 2011), Chap. 10.

[26] L. Seabra, P. Sindzingre, T. Momoi, and N. Shannon, Phys. Rev. B **93**, 085132 (2016).

[27] M. Goto, H. Ueda, C. Michioka, A. Matsuo, K. Kindo, K. Sugawara, S. Kobayashi, N. Katayama, H. Sawa, and K. Yoshimura, Phys. Rev. B **97**, 224421 (2018).

[28] E. Parker and L. Balents, Phys. Rev. B **95**, 104411 (2017).

[29] V. S. Abgaryan, N. S. Ananikian, L. N. Ananikyan, and V. V. Hovhannisyan, Solid State Commun. **224**, 15 (2015).

[30] H. Nakano and T. Sakai, J. Phys. Soc. Jpn. **84**, 063705 (2015).

[31] O. Götze, J. Richter, R. Zinke, and D. J. J. Farnell, J. Magn. Magn. Mater. **397**, 333 (2016).

[32] T. Liu, W. Li, and G. Su, Phys. Rev. E **94**, 032114 (2016).

[33] K. Morita, T. Sugimoto, S. Sota, and T. Tohyama, Phys. Rev. B **97**, 014412 (2018).

[34] K. Jia, C.-X. Wang, X. Dong, N. Chen, J. Cong, G. Li, H. L. Feng, H. Zhao, and Y. Shi, Phys. Rev. Res. **3**, 043178 (2021).

[35] J. A. M. Paddison, G. Ehlers, A. B. Cairns, J. S. Gardner, O. A. Petrenko, N. P. Butch, D. D. Khalyavin, P. Manuel, H. E. Fischer, H. Zhou *et al.*, npj Quantum Mater. **6**, 99 (2021).

[36] S. A. M. Mentink, A. Drost, G. J. Nieuwenhuys, E. Frikkee, A. A. Menovsky, and J. A. Mydosh, Phys. Rev. Lett. **73**, 1031 (1994).

[37] A. Dönni, G. Ehlers, H. Maletta, P. Fischer, H. Kitazawa, and M. Zolliker, J. Phys.: Condens. Matter. **8**, 11213 (1996); V. Fritsch, S. Lucas, Z. Huesges, A. Sakai, W. Kittler, C. Taubenheim, S. Woitschach, B. Pedersen, K. Grube, B. Schmidt *et al.*, J. Phys.: Conf. Ser. **807**, 032003 (2017); A. Oyamada, S. Maegawa, M. Nishiyama, H. Kitazawa, and Y. Isikawa, Phys. Rev. B **77**, 064432 (2008); S. Lucas, Phys. Rev. Lett. **118**, 107204 (2017).

[38] S. K. Upadhyay, K. K. Iyer, and E. V. Sampathkumaran, J. Phys.: Condens. Matter. **29**, 325601 (2017); E. V. Sampathkumaran, K. K. Iyer, S. K. Upadhyay, and A. V. Andreev, Solid State Commun. **288**, 64 (2019).

[39] M. He, X. Xu, Z. Wu, C. Dong, Y. Liu, Q. Hou, S. Zhou, Y. Han, J. Wang, and Z. Qu, Phys. Rev. Mater. **7**, 033401 (2023).

[40] Y. Chen, Y. Zhang, R. Li, H. Su, Z. Shan, M. Smidman, and H. Yuan, Phys. Rev. B **107**, 094414 (2023).

[41] B. Chevalier, P. Lejay, J. Etourneau, and P. Hagenmuller, Solid State Commun. **49**, 753 (1984).

[42] See Supplemental Material at http://link.aps.org/supplemental/10.1103/PhysRevMaterials.7.L101401 for experimental methods, crystallographic information, Rietveld fitting of the x-ray-diffraction pattern, and the magnetic susceptibility behavior at some low fields around the magnetic transition for Er_2RhSi_3.

[43] K. Mukherjee, T. Basu, K. K. Iyer, and E. V. Sampathkumaran, Phys. Rev. B **84**, 184415 (2011).

[44] M. Smidman, C. Ritter, D. T. Adroja, S. Rayaprol, T. Basu, E. V. Sampathkumaran, and A. D. Hillier, Phys. Rev. B **100**, 134423 (2019).

[45] K. Maiti, T. Basu, S. Thakur, N. Sahadev, D. Biswas, G. Adhikary, Y. Xu, W. Löser, and E. V. Sampathkumaran, J. Phys.: Condens. Matter **32**, 46LT02 (2020).

[46] R. Mallik, E. V. Sampathkumaran, M. Strecker, and G. Wortmann, Europhys. Lett. **41**, 315 (1998).

[47] Z. Wang, K. Barros, G.-W. Chern, D. L. Maslov, and C. D. Batista, Phys. Rev. Lett. **117**, 206601 (2016).

[48] S. R. Saha, H. Sugawara, T. D. Matsuda, H. Sato, R. Mallik, and E.V. Sampathkumaran, Phys. Rev. B **60**, 12162 (1999).

[49] E. V. Sampathkumaran, arXiv:1910.09194.

[50] T. Kurumaji, T. Nakajima, M. Hirschberger, A. Kikkawa, Y. Yamasaki, H. Sagayama, H. Nakao, Y. Taguchi, T. Arima, and Y. Tokura, Science **365**, 914 (2019).

[51] J. A. M. Paddison, B. K. Rai, A. F. May, S. Calder, M. B. Stone, M. D. Frontzek, and A. D. Christianson, Phys. Rev. Lett. **129**, 137202 (2022).

[52] T. Nomoto and R. Arita, J. Appl. Phys. **133**, 150901 (2023).

[53] R. Mallik, E. V. Sampathkumaran, and P. L. Paulose, Solid State Commun. **106**, 169 (1998).

[54] S. Majumdar, E. V. Sampathkumaran, P. L. Paulose, H. Bitterlich, W. Loser, and G. Behr, Phys. Rev. B **62**, 14207 (2000).

[55] P. L. Paulose, E. V. Sampathkumaran, H. Bitterlich, G. Behr, and W. Löser, Phys. Rev. B **67**, 212401 (2003).

[56] K. K. Iyer, P. L. Paulose, E. V. Sampathkumaran, M. Frontzek, A. Kreyssig, M. Doerr, M. Loewenhaupt, I. Mazilu, G. Behr, and W. Löser, Physica B **355**, 158 (2004).

[57] W. Bazela, E. Wawrzynska, B. Penc, N. Stusser, A. Szytula, and A. Szygmunt, J. Alloys Compd. **360**, 76 (2003).

[58] R. E. Gladyshevskii, K. Cenzual, and E. Parthe, J. Alloys Compd. **189**, 221 (1992).

[59] I. Das and E. V. Sampathkumaran, J. Magn. Magn. Mater. **137**, L239 (1994).

[60] J. Leceijewicz, N. Stüsser, A. Szytula, and A. Szygmunt, J. Magn. Magn. Mater. **147**, 45 (1995).

[61] M. Szlawska, D. Kaczorowski, A. Slebarski, L. Gulay, and J. Stepien-Damm, Phys. Rev. B **79**, 134435 (2009).

[62] N. Kase, T. Muranaka, and J. Akimitsu, J. Magn. Magn. Mater. **321**, 3380 (2009).

[63] T. Nakano, K. Sengupta, S. Rayaprol, M. Hedo, Y. Uwatoko, and E. V. Sampathkumaran, J. Phys.: Condens. Matter **19**, 326205 (2007).

[64] S. Patil, K. K. Iyer, K. Maiti, and E. V. Sampathkumaran, Phys. Rev. B **77**, 094443 (2008).

[65] S. Patil, V. R. R. Medicherla, R. S. Singh, S. K. Pandey, E. V. Sampathkumaran, and K. Maiti, Phys. Rev. B **82**, 104428 (2010).

[66] S. Patil, V. R. R. Medicherla, R. S. Singh, E. V. Sampathkumaran, and K. Maiti, Europhys. Lett. **97**, 17004 (2012).

[67] K. Mukherjee, K. K. Iyer, S. Patil, K. Maiti, and E. V. Sampathkumaran, J. Phys.: Conf. Ser. **273**, 012010 (2011).

[68] R. Kumar, K. K. Iyer, P. L. Paulose, and E. V. Sampathkumaran, Phys. Rev. B **101**, 144440 (2020).

[69] Initial magnetization results were presented in *Proceedings of the DAE Solid State Physics Symposium*, (Ranchi, 2022), edited by A. K. Mishra, M. Tyagi, and D. V. Udupa (AIP, Melville, 2022), Vol. 56.

[70] N. Marcano, J. C. Gómez Sal, J. L. Espeso, L. Fernández Barquín, and C. Paulsen, Phys. Rev. B **76**, 224419 (2007); T. D. Yamamoto, A. Kotani, H. Nakajima, R. Okazaki, H. Taniguchi, S. Mori, and I. Terasaki, J. Phys. Soc. Jpn. **85**, 034711 (2016); D. X. Li, S. Nimori, Y. Shiokawa, Y. Haga, E. Yamamoto, and Y. Onuki, Phys. Rev. B **68**, 172405 (2003).

[71] R. Kumar, J. Sharma, K. K. Iyer, and E. V. Sampathkumaran, J. Magn. Magn. Mater. **490**, 165515 (2019).

[72] J. A. Mydosh, *Spin Glasses: An Experimental Introduction* (Taylor & Francis, London, 1993).

[73] K. A. Gschneidner, V. K. Pecharsky, Jr., and A. O. Tsokol, Rep. Prog. Phys. **68**, 1479 (2005).

[74] R. Mallik and E. V. Sampathkumaran, Phys. Rev. B **58**, 9178 (1998).

[75] R. Kumar and E. V. Sampathkumaran, J. Magn. Magn. Mater. **538**, 168285 (2021), and references therein.

[76] M. W. Butcher, M. A. Tanatar, and A. H. Nevidomskyy, Phys. Rev. Lett. **130**, 166701 (2023).

[77] A. Silveira, R. Erichsen, Jr., and S. G. Magalhaes, Phys. Rev. E **103**, 052110 (2021).

[78] A. Szytula, M. Hofmann, B. Penc, M. Slaski, S. Majumdar, E. V. Sampathkumaran, and A. Zygmunt, J. Magn. Magn. Mater. **202**, 365 (1999).

[79] M. Frontzek, A. Kreyssig, M. Doerr, A. Schneidewind, J.-U. Hoffmann, and M. Loewenhaupt, J. Phys.: Condens. Matter **19**, 145276 (2007).

[80] S. Niitaka, K. Yoshimura, K. Kosuge, M. Nishi, and K. Kakurai, Phys. Rev. Lett. **87**, 177202 (2001).

[81] M. Loewenhaupt, W. Schafer, A. Niazi, and E. V. Sampathkumaran, Europhys. Lett. **63**, 374 (2003).